

Electro-mechanical impedance based strength monitoring technique for hydrating blended cements

Thirumalaiselvi, A.* and Saptarshi Sasmal

Special and Multifunctional Structures Laboratory, CSIR-Structural Engineering Research Centre, Taramani, Chennai-600113, India

(Received November 11, 2019, Revised January 27, 2020, Accepted January 28, 2020)

Abstract. Real-time monitoring of stiffness and strength in cement based system has received significant attention in past few decades owing to the development of advanced techniques. Also, use of environment friendly supplementary cementitious materials (SCM) in cement, though gaining huge interest, severely affect the strength gain especially in early ages. Continuous monitoring of strength- and stiffness- gain using an efficient technique will systematically facilitate to choose the suitable time of removal of formwork for structures made with SCM incorporated concrete. This paper presents a technique for monitoring the strength and stiffness evolution in hydrating fly ash blended cement systems using electro-mechanical impedance (EMI) based technique. It is important to observe that the slower pozzolanic reactivity of fly ash blended cement systems could be effectively tracked using the evolution of equivalent local stiffness of the hydrating medium. Strength prediction models are proposed for estimating the strength and stiffness of the fly ash cement system, where curing age (in terms of hours/days) and the percentage replacement of cement by fly ash are the parameters. Evaluation of strength as obtained from EMI characteristics is validated with the results from destructive compression test and also compared with the same obtained from commonly used ultrasonic wave velocity (UPV). Statistical error indices indicate that the EMI technique is capable of predicting the strength of fly ash blended cement system more accurate than that from UPV. Further, the correlations between stiffness- and strength- gain over the time of hydration are also established. From the study, it is found that EMI based method can be effectively used for monitoring of strength gain in the fly ash incorporated cement system during hardening.

Keywords: impedance; hydration; fly ash blended cement; ultrasonics; strength gain; stiffness

1. Introduction

Development of green (eco-friendly by reducing cement consumption) blended/engineered cement composite system using supplementary cementitious materials (SCMs) is an ever demanding research area due to its immense environmental impact. Among the SCMs available, fly ash is the most widely used supplementary material, owing to its abundant availability, compatibility and low cost. Fly ash is a by-product of the combustion of coal in thermal power plants (Thomas 2007) and primarily comprises of silicon and aluminium oxides (Prem *et al.* 2019). Advantage of incorporation of fly ash into cement system is two-fold: one by minimizing the detrimental environmental effect caused by cement production; in other way by effectively re-using the waste by-product. However, its addition in cement system is found to have adverse effects on the early age strength development due to drastic change in hydration process (Hassett and Eylands 2007, Lam *et al.* 2000, Sakai *et al.* 2005, Şahmaran *et al.* 2007, Hemalatha and Sasmal 2018). This problem is highly relevant in situations such as removal of formwork at construction site, post-tensioning of prestressing tendons, etc. where desired early age strength

should be achieved (Bhalla *et al.* 2018). Thus, it is of great importance to monitor the material characteristics (in terms of key mechanical properties) like stiffness and strength (especially compressive strength which is crucial from design aspect) gain of such blended composite systems during the hardening process.

Towards this, many investigations were carried out to study the strength development of cement system containing fly ash. Over the years, strength gain in fly ash replaced cement composite system at different ages of curing is obtained by conducting the compression tests on cube or cylinder specimens (Sata *et al.* 2007, Namagga and Atadero 2009, Hemalatha and Sasmal 2018). Besides the conventional destructive tests, few researchers attempted to correlate the strength gain with the degree of hydration reaction (Shafiq 2011, Sofi *et al.* 2017). Heat of hydration obtained from isothermal calorimetry was correlated with compressive strength for fly ash blended cement specimens (Tanesi and Ardani 2013). However, its application is limited for the examination of strength gain at very early age when the heat release rate is predominant.

Among the various advanced techniques, wave propagation based techniques such as ultrasonic pulse velocity (UPV) test, rebound hammer test, pulse-echo method, ground penetrating radar method, etc. are very common for concrete structures. Specifically, UPV based techniques are being used for testing of concrete structure for many decades as the technique is simple and user

*Corresponding author, Scientist,
E-mail: selvi@serc.res.in

friendly. Evaluation of the strength of hardened cement/concrete system using ultrasonic wave propagation is well reported and matured area of research (Galan 1967, Tharmaratnam and Tan 1990, Neville 1995, Qixian and Bungey 1996, Lin *et al.* 2003, Demirboğa *et al.* 2004, Gül *et al.* 2006, Trtnik *et al.* 2009, Ji *et al.* 2015, Zhang *et al.* 2018). Thus, it is not discussed again in this study. However, the interest on tracing strength gain over the period of hydration of concrete and any change in the phenomenon due to alteration/incorporation in the pozzolanic constituent(s) by employing the truly non-destructive manner have gained substantial interest in the recent years. Lim *et al.* (2016) proposed a procedure to monitor the development of elastic properties during hardening of concrete from day 1 to 28 using the piezoelectric (PZT) sensors based wave propagation technique. Wolfs *et al.* derived the relation between ultrasonic velocity measurements and compressive strength of 3D printed objects in the fresh material state (Wolfs *et al.* 2018). An empirical formula was proposed by Yoon *et al.* (2017) for evaluating the early-age compressive strength of concrete using surface wave velocity measurements.

Electro-mechanical impedance (EMI) based wave propagation technique was explored by few researchers in recent times, for strength and damage monitoring as the required sensors are cheap, implementation is simple and suiting the requirement of continuous monitoring (Soh and Bhalla 2005, Rajabi *et al.* 2017, Huynh *et al.* 2018, Kang *et al.* 2018). Application of EMI technique for strength estimation is first studied by Soh and Bhalla (2005). They observed that the first peak frequency gradually shifts with the gain in concrete strength. They also proposed an empirical relationship between concrete strength and the first resonant frequency. Shin *et al.* (2008) found that the resonant frequency shift index, strength gain index, root mean-square deviation (RMSD) values have a strong correlation for all curing conditions. Tawie and Lee (2010) showed that the strength gain of concrete can be monitored using the resonant frequency shift and statistical parameters such as RMSD, mean absolute percentage deviation (MAPD) and cross correlation deviation (CCD) values. Wang and Zhu (2011) proposed the correlations between concrete strength development and RMSD, MAPD. Quinn *et al.* (2012) proposed an embedded wireless monitoring system for tracking initial curing and strength of concrete structures. Mechanical impedance was extracted from the measured admittance signatures by Wang *et al.* (2014). They brought out that the cross correlation index-based mechanical impedance is highly sensitive to variation in the concrete compressive strength. Kim *et al.* (2014) applied impedance measuring technique to monitor the curing process. Impedance signals measured and the strength evaluated through destructive tests were used to develop the estimation equation. Saravanan *et al.* (2015, 2017) observed rightward shifting of the peak frequency due to increase in the stiffness and the upward shifting of amplitudes as curing proceeds. Lim *et al.* (2016) reported an interesting fact that the resonance of PZT patch doesn't give proper indication of the concrete stiffness, since it is highly influenced by the surrounding boundary conditions of the PZT patch.

Talakokula *et al.* (2018) reported a study where PZTs were bonded on rebars and the same was embedded inside concrete to monitor concrete hydration. They found that the equivalent stiffness reflects the stiffness development during hydration. Few have attempted to apply wave propagation methods for monitoring the hydration process in blended cement system containing fly ash (Lee *et al.* 2004, Lu *et al.* 2015, Zheng *et al.* 2018 and Mohammed and Adamu 2018, Ghafari *et al.* 2018).

In spite of considerable number of related works including those mentioned above, studies focussing on the evaluation of stiffness and strength gain properties on the cement system using electro-mechanical impedance technique are very scanty. Nevertheless it is true that the EMI technique is easy to employ, non-invasive, and fit for continuous monitoring unlike many other non-destructive techniques. To the authors knowledge, no attempt has yet been made to explore the EMI technique for monitoring the mechanical properties of fly ash incorporated cement system where determining the strength and stiffness at early age is extremely crucial. This could be very effective to bring a comprehensive measurement technique to track the hydration (hardening) in blended cement systems in newly constructed structures. The novelty of the present study is, firstly in characterizing the admittance signature and direct evaluation of local stiffness in fly ash incorporated concrete during the process of hydration. Further, the present study focuses on investigating the efficacy of impedance characteristics for indirect evaluation of strength gain of fly ash incorporated concrete. The predicted strength is thoroughly validated with destructive tests and also compared with the ultrasonic wave velocity studies. Since, strength is a very common and conceivable design parameter and stiffness reflects the integrity of structure, it signifies the need for establishing the correlation between stiffness (direct evaluation from EMI) and strength (indirect evaluation from EMI). Addition of fly ash significantly influences the change in the strength gain and thus, the strength and stiffness properties will be very different from any normal concrete. In view of this, the present study is also aimed at correlating the stiffness and strength of the fly ash incorporated cement system, evaluated using EMI technique.

2. Experimental program

2.1 Materials

Three cement composite mixes, proportioned (by weight) with or without fly ash were prepared as shown in Table 1. Water to binder ratio of 0.3 was kept constant while

Table 1 Composition of cement composites

Mix No.	Mix name	Cement	Fly ash	w/b ratio
1	CP_0	1	-	0.3
2	CP_20	0.8	0.2	0.3
3	CP_40	0.6	0.4	0.3

in mixes 2 and 3, cement was replaced with fly ash by 20% and 40%, respectively. 53 grade ordinary Portland cement of IS:4031 (1968), fly ash conforming to ASTM C618-8a (2013) and normal tap water were used in this study.

2.2 Mix proportion and specimen preparation

Prism specimens dimensioned 100 mm×100 mm×500 mm were cast in metal moulds using each mix. For each type of mix, two measurements (UPV and EMI) were done on same specimen. The longitudinal sides of metal moulds were removed after 5hr of casting for carrying out UPV measurement. 18 numbers of 100 mm (length) × 200 mm (diameter) cylinder specimens were also prepared for each mix for the determination of compressive strength at 1 day, 2 days, 3 days, 7 days, 14 days and 28 days of curing. Three cylinder specimens for each mix were demoulded after 24 h and cured in water for 28 days before the destructive compression test.

3. Impedance using piezoelectric EMI tests

The EMI technique is similar to the global dynamic response techniques with the only difference being the frequency range employed, which is typically 10-900 kHz in EMI technique, against less than 100 Hz as in the case of the conventional dynamic methods for structures (Soh and Bhalla 2005). EMI technique utilizes a PZT patch which is bonded using adhesive onto the surface of the host structure to be monitored, and excited electrically through an impedance analyser. Excitation is done by applying alternating voltage after proper setting of adhesive-PZT. The PZT patch-host structure system can be modelled in a simplified way as a mechanical impedance (due the host structure) connected to vibrating PZT patch (Fig. 1) (Liang *et al.* 1997, Bhalla 2004, Huynh and Kim 2017). The differential equation to describe the one-dimensional vibration of the PZT patch is derived using the following dynamic equilibrium, as given by (Bhalla *et al.* 2012)

$$\bar{Y}_E \frac{\partial^2 u}{\partial x^2} = \rho \frac{\partial^2 u}{\partial t^2} \quad (1)$$

where u is the displacement, $\bar{Y}_E (= Y^E(1 + \eta j))$ is the complex modulus of elasticity of PZT at constant electric field, ρ is the density, x and t represent the space and time.

Solving this, expression for the coupled electro-mechanical admittance can be derived as (Talakokula *et al.* 2018)

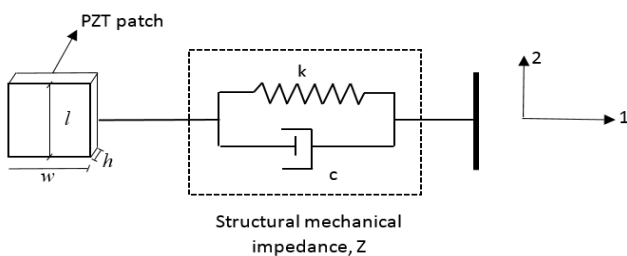


Fig. 1 One-dimensional impedance model

$$Y = G + Bj \\ = \omega j \frac{wl}{h} \left[\bar{\epsilon}_{33}^T - d_{31}^2 \bar{Y}^E + \left(\frac{Z_a}{Z + Z_a} \right) d_{31}^2 \bar{Y}^E \left(\frac{\tan \kappa l}{\kappa l} \right) \right] \quad (2)$$

where G is the conductance (real part of admittance), B is the susceptance (imaginary part of admittance), $\omega (= 2\pi f)$ is the angular frequency, w , l , h are PZT dimensions, $\bar{\epsilon}_{33}^T (= \epsilon_{33}^T(1 - \delta j))$ is the complex electrical permittivity, $\bar{Y}^E (= Y^E(1 + \eta j))$ is the complex modulus of elasticity, κ is wave number ($= \omega \sqrt{\frac{\rho}{Y^E}}$), d_{31} is the piezoelectric strain coefficient, Z and Z_a are the mechanical impedance of the system and PZT, respectively, η and δ are the mechanical and dielectric loss factors respectively.

In the present study, Agilent 4294A precision impedance analyser was used for acquiring the admittance signatures throughout the hardening process. SP-5H PZT patches of size 10 mm (w) × 10 mm (l) × 0.25 mm (h), manufactured by Sparkler Ceramics Pvt. Ltd were used in the present study. The PZTs were affixed on the top surface of the specimens using quick set epoxy after 6 hours of casting (when the specimen surface is sufficiently dry to affix the PZT). Two such PZTs were bonded onto the surface of each specimen at specific distance to ensure the repeatability in acquired admittance signatures (Fig. 2). In addition, to reduce noise, the signatures were acquired with five repeated measurements and averaged. The electrical- and mechanical- properties of the PZT transducers as provided by the manufacturer are listed in Table 2. An alternating voltage of 500 mV was applied across the PZT transducer and admittance signature was recorded in the frequency range of 40-900 kHz. Admittance signatures were acquired after the PZTs were bonded. Acquisition was done at every one hour on the 1st day (as hydration reaction is very fast during that time) and thereafter, once a day till 14th day. Beyond 14 days, admittance signatures were recorded at 21st day, 26th day and 28th day. All the tests were performed under temperature and humidity controlled laboratory conditions (26^o Celsius temperature and 75-80% humidity). Though the electrical admittance signatures acquired from the impedance analyser are reported to be temperature sensitive in the present study, all the observations are made from the active part of measured admittance signature and the active part is found to have superior tolerance to temperature fluctuations. Experimental setup comprising of impedance analyser, computer equipped with data capturing software, GPIB interface cable, PZT attached specimen, are presented in Fig. 3.



Fig. 2 Instrumentation using PZT for acquiring the impedance from cement composite specimens

Table 2 Properties of PZT transducers

Property	Values
Density, ρ (kg/m ³)	7500
Young's Modulus, Y^E (N/m ²)	6.67E10
Electric Permittivity, ϵ_{33}^T (farad/m)	2.603e-8
Piezoelectric Strain Coefficient, d_{31} (m/V)	-2.65E-10
Dielectric loss factor, δ	0.0129
Mechanical loss factor, η	0.044

4. Experimental results

4.1 Prediction of stiffness properties during hardening from EMI technique

Typical admittance (real part-conductance, G; and imaginary part-susceptance, B) signature measured in cement composite mixes at age of 1 day is shown in Fig. 4. It is commonly noticed from all the composites that first resonance peak occurs in the frequency range of 100-300 kHz. Also, it is observed from Fig. 5 that, when the cement system is getting hydrated, there is a significant change in admittance signature due to the change in the host structural parameter. It has been reported in earlier studies that as hydration proceeds, conductance curve shifts to the right due to the increase in structural stiffness (Lee *et al.* 2004, Soh and Bhalla 2005, Shin *et al.* 2008, Tawie and Lee 2010, Saravanan *et al.* 2015, 2017, Talakokula *et al.* 2018). Similar behaviour is also observed from the present investigations, even for the fly ash blended system (see Fig. 5). However, for quantitative estimation of stiffness development during hydration, the method proposed by Balla (2004) is employed in the present study. Structural (i.e., cement system) impedance components are derived from the experimentally measured admittance signature and using analytical expression for coupled electro-mechanical admittance (given by Eq. (2)). For easier understanding, few salient steps are explained below.

Following Eq. (2), the electro-mechanical admittance can be deconstructed into two parts as follows

$$Y = \omega j \frac{wl}{h} [\epsilon_{33}^T - d_{31}^2 \bar{Y}^E] + \omega j \frac{wl}{h} \left[\left(\frac{Z_a}{Z + Z_a} \right) d_{31}^2 \bar{Y}^E \left(\frac{\tan kl}{kl} \right) \right] \quad (3)$$

Part 1-Passive

Part 2-Active

As observed from Eq. (3), passive part (Y_P) is dependent only on the PZT patch parameters whereas active part (Y_A) involves the contribution from both PZT and host structure. From the known PZT parameters, Y_P can be easily obtained and thus, it can be subtracted from the experimentally measured admittance signature to finally obtain the active part. However, at times, some of PZT parameters may not be same as those provided by the manufacturer. Usage of

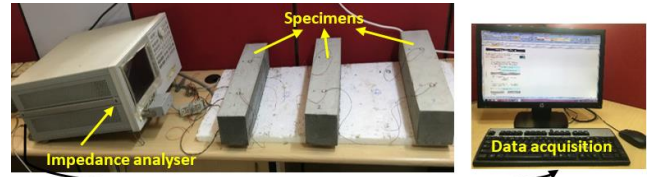


Fig. 3 EMI-based wave propagation experimental setup

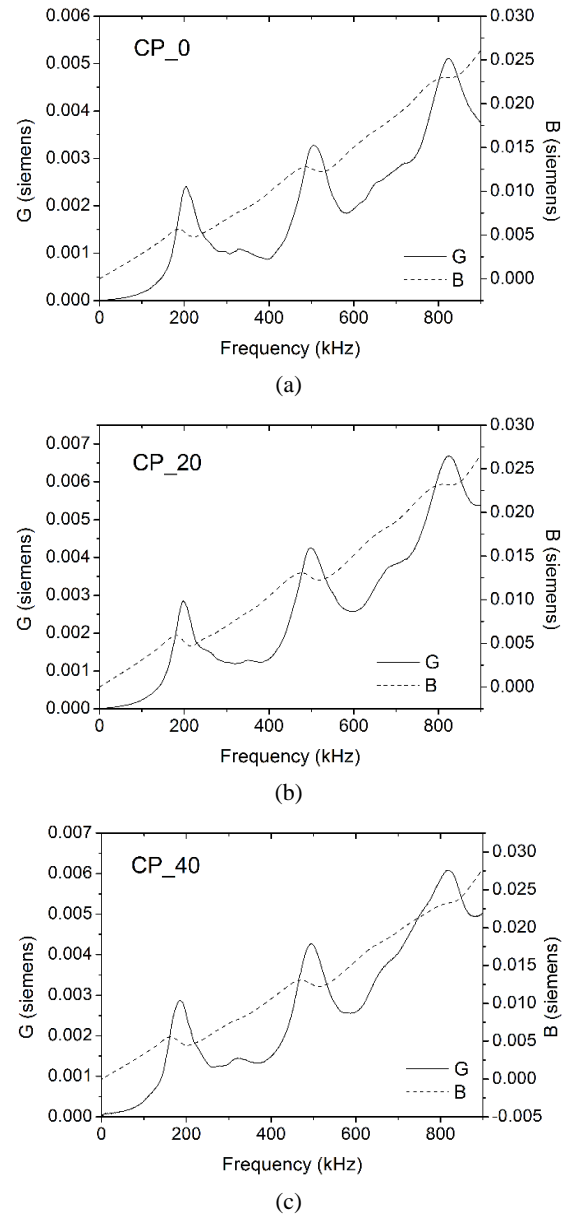


Fig. 4 Typical admittance signature observed in different composites. (a) CP_0; (b) CP_20; (c) CP_40

correct PZT parameters is very important since the prediction of structural impedance depends mainly on the PZT parameters. For this sake, it is recommended that the admittance signatures of the PZT patches need to be measured in the 'free-free' condition before attaching them to the host structure at very low excitation frequencies (as proposed by Bhalla 2004). Under such low excitations

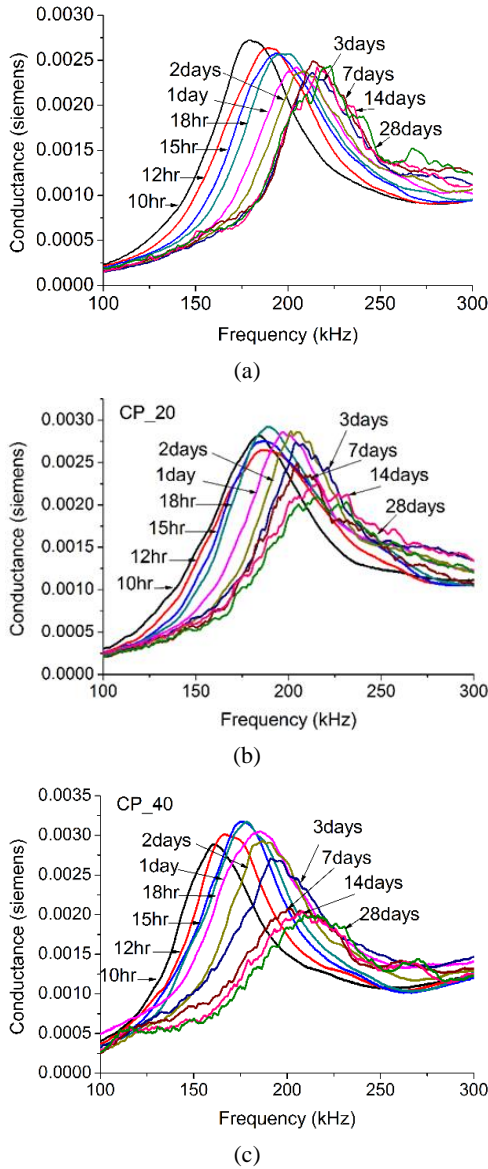


Fig. 5 Conductance signatures obtained in the frequency range of 100-300 kHz. (a) CP_0; (b) CP_20; (c) CP_40

typically less than one-fifth of the first resonance frequency of the PZT patch, $\left(\frac{\tan kl}{kl}\right) \rightarrow 0$, PZT electrical parameters ϵ_{33}^T and δ can be determined.

From the free state studies, ϵ_{33}^T is found to be $2.603E-8$ F/m for SP-5H PZT (against a value of $2.12E-8$ F/m supplied by the manufacturer). Similarly, δ was found out to be 0.0129, against a value of 0.015 provided by the supplier. To get sufficient confidence upon the PZT parameters, from Eq. (3) free admittance signatures of the PZT patch is obtained in the 'free-free' condition in the frequency range 40 Hz-900 kHz, using the obtained values of the PZT parameters and compared with the experimentally measured 'free-free' condition (shown in Fig. 6). Some discrepancies do exist which need further fine tuning of the PZT parameters. Generally, it is observed that the experimentally measured resonance frequency is on the higher side than the frequency computed analytically. Also, experimental

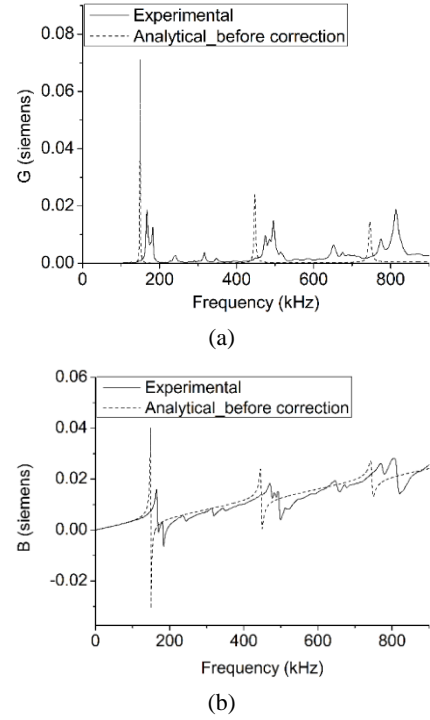


Fig. 6 Comparison of PZT patch admittance signatures in the frequency range of 40 Hz to 900 kHz in free-free condition. (a) Conductance variation; (b) Susceptance variation

conductance and susceptance values are lower than those obtained analytically as reported in earlier studies (Bhalla 2004).

While arriving at the suitable PZT parameter that can fit well with the experimentally obtained admittance signatures, method proposed in Bhalla (2004) is used. A correction factor, C is introduced in the term $(\tan kl/kl)$ to match the resonant frequency and $C = 0.89$ is found by trial and error, so that the term $(\tan kl/kl)$, can now be replaced by $(\tan Ckl/Ckl)$. Further, η is found out to be 0.044 (using trial and error approach) for enabling better match between the experimental and the analytical values of admittance signatures. Fig. 7 compares the analytical signatures based on the modified PZT parameters (after updating PZT model) and the experimental signatures. Good agreement is found between the two which give sufficient confidence to proceed further with the modified parameters for structural impedance evaluation.

Now, with the corrected PZT parameters, Y_P (PZT contribution alone) can be determined and removed from the experimentally measured admittance signature to get active part for structural impedance evaluation. Substituting $\bar{\epsilon}_{33}^T = \epsilon_{33}^T(1 - \delta j)$, $\bar{Y}^E = Y^E(1 + \eta j)$, $(\tan kl/kl) = (\tan Ckl/Ckl) = r + tj$, active part in Eq. (7) is rewritten as

$$\begin{aligned} Y_A &= G_A + B_A j \\ &= \omega j \frac{wl}{h} \left[\left(\frac{Z_a}{Z + Z_a} \right) d_{31}^2 Y^E (1 + \eta j) (r + tj) \right] \\ &= \omega j \frac{wl}{h} \left(\frac{Z_a}{Z + Z_a} \right) d_{31}^2 Y^E (R + Tj) \end{aligned} \quad (4)$$

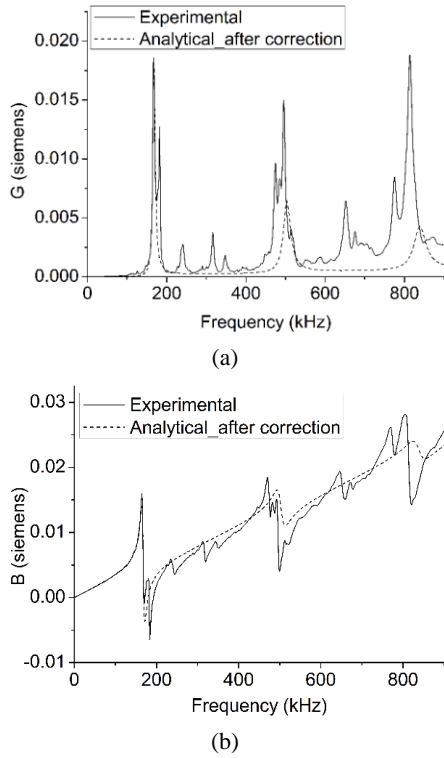


Fig. 7 Comparison of PZT patch admittance signatures in the frequency range of 40 Hz to 900 kHz in free-free condition after incorporating modified parameters. (a) Conductance variation; (b) Susceptance variation

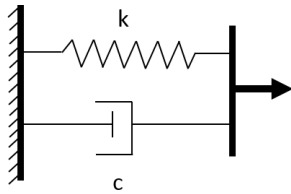


Fig. 8 Identified equivalent system

where $R = r - \eta t$ and $T = \eta r + t$.

Structural impedance varying over the hydration process, contains the information to describe the characteristics of the hydrating blended cement composite medium. To explain the characteristics of the evolving hydrating medium such as stiffness, an equivalent structural system is identified. In the frequency range of 50-100 kHz, real part of structural impedance is found to be more or less constant, however, the imaginary part is found to be decreasing with the increase in frequency. This behaviour is similar to the Kelvin-Voigt system (parallel arrangement of stiffness and damper) as schematically shown in Fig. 8. Similar equivalent system is proposed in Bhalla *et al.* (2012), Talakokula *et al.* (2018) for other applications.

The real and imaginary components of Kelvin-Voigt system are described as

$$\begin{aligned} x &= c \\ y &= -\frac{k}{\omega} \end{aligned} \quad (5)$$

Within the frequency range 50-100 kHz, variation of real and imaginary parts of structural impedance is illustrated in Fig. 9 for typical case (say CP_0 at day 9). Corresponding values of parameters c and k are also defined in the same figure.

Similarly, stiffness parameter of the identified equivalent system is evaluated throughout the hardening process from 7 hrs of casting till 28 days using the Eq. (5) for all the specimens. Fig. 10 shows the variation of equivalent local stiffness at different ages of curing of cement composite medium. As expected, equivalent stiffness, ' k ' is high in pure cement system compared to fly ash blended systems. In addition, ' k ' keeps increasing, with sharp increase till day 1 (denoted by point 'A'). Beyond which the rate of increase in ' k ' slows down. Stiffness increase reaches a plateau faster (point 'B') in pure cement system (CP_0) approximately in 7 days. It takes more time for the fly ash blended systems to attain stable (14 days for CP_20 and 22 days for CP_40). This again due to the slower pozzolanic reaction as seen in velocity evolution (section 4.1.1). From this, it can be concluded that

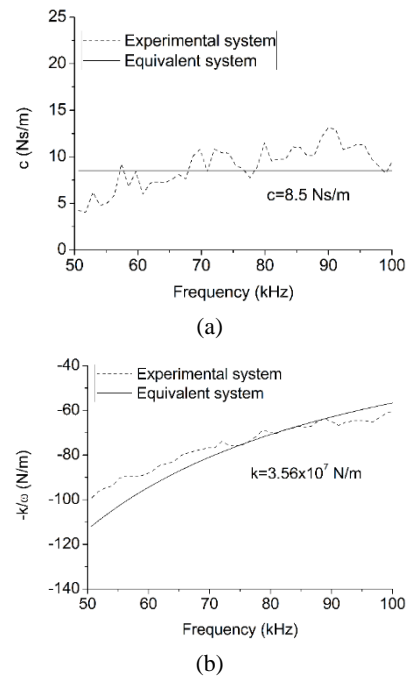


Fig. 9 Comparison of experimental and equivalent plots

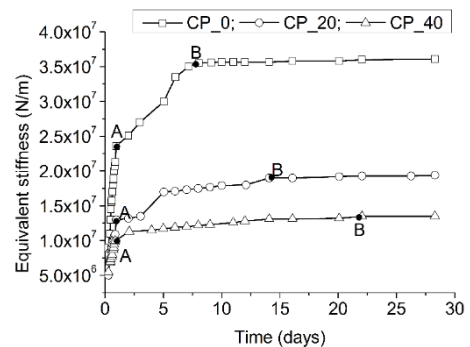


Fig. 10 Equivalent local stiffness

impedance based approach can be considered as a powerful tool to monitor and assess the hydration of cement based medium in any structural system. It is also to note that the observation on gain in equivalent stiffness for different cement system during the process of hardening is typically shown here for a certain frequency range (50–100k Hz). In other frequency range, this absolute value will differ.

4.2 Evaluation of strength gain during hardening of fly ash blended cement system

4.2.1 Destructive compression test

Experiments were carried out in order to determine the mechanical properties (strength, Young's modulus and Poisson's ratio) of the prepared cement composite mixes (pure and fly ash blended) at 1 day, 2 days, 3 days, 7 days, 14 days and 28 days of curing age. Three cylinder specimens for each mix were cast and tested. Compression tests on cement composites were performed using hydraulic controlled compression test machine of 3000 kN capacity. Additionally, 475 kN load cell was used to capture the actual load exerted to the specimens. Multi-channel high speed digital data acquisition system (DAQ) QuantumX was used to acquire the strain and load information from the specimen. For measuring lateral strain, 120 Ω electric resistant strain gauges of 30 mm gauge length was pasted in horizontal (along the periphery of the specimen) direction at mid-height of each specimen. To measure the longitudinal strain, three 120 Ω strain gauges, each of 30 mm gauge length, were attached vertically (along the height of the specimen) in mid-height of the specimen, 120° apart. The strain gauges were glued to the specimen surface with special type of conductive adhesive. Strain gauge readings (lateral and longitudinal strain) were recorded using the 16-channel strain gauge module connected to the DAQ with sampling frequency of 10 Hz.

For determining the Young's modulus of the specimens, two loading-unloading cycles were performed under load control, with a constant loading rate of 500 N/s. First, the compressive load level was increased from the zero to 30% of assumed peak load capacity and unloaded. The same was

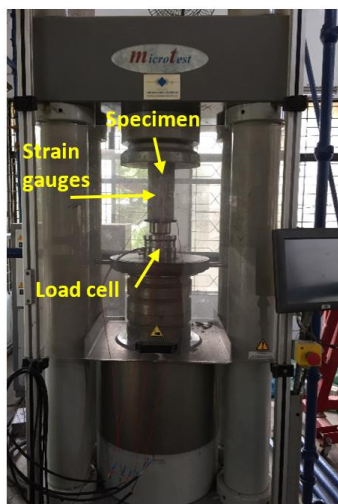


Fig. 11 Compression test set-up

repeated and finally, the load was increased till the specimen reached its failure stage. Poisson's ratio is determined by taking the average values of the ratio of lateral strain to the longitudinal strain measured at different load levels. Typical experimental setup is shown in Fig. 11.

4.2.2 Strength gain from EMI technique

It is also commonly noticed in all blended system (as depicted in Fig. 5) that shift in peak frequency towards right when the cement medium hydrates. This shift is attributed to the increase in medium stiffness during hardening (as seen demonstrated in previous section). Also stiffening behaviour can be related to the increase in strength during hardening. Though the first peak frequency occurs in the frequency range of 100-300 kHz in all cement composites, exact values of peak frequency differ with the type of composite medium. Plot between first resonant frequency at particular curing age and compressive strength measured experimentally corresponding to that age is shown in Fig. 12. Based on the plot, following empirical relation is proposed using exponential curve fitting which can be used for predicting the early age strength of fly ash blended cement system

$$f_{cu} = A * e^{0.043 * f_{peak}} \quad (6)$$

where the factor 'A' depends on percentage of fly ash (A equals, 0.00401 for CP_0; 0.00472 for CP_20; 0.0048 for CP_40).

From the peak frequency values which shift during hardening, compressive strength is estimated using the above derived empirical relations (see Fig. 13). Good agreement is found between the experimental and predicted strength values. It is to note that the peak frequency depends primarily on the type of material, however geometry of PZT and bond also play a role. Hence these relations are applicable only to the materials considered for the present study, which is the main limitation. However to make it applicable to different cement systems similar methodology can be followed.

4.2.3 Strength gain from ultrasonic tests

The ultrasonic experiments were also done to monitor the strength development by measuring the wave velocity at different ages of curing. Two 23 mm diameter ultrasonic transducers PA956 (manufactured by Precision Acoustics Ltd.) were used. Grease was used as a couplant to attach

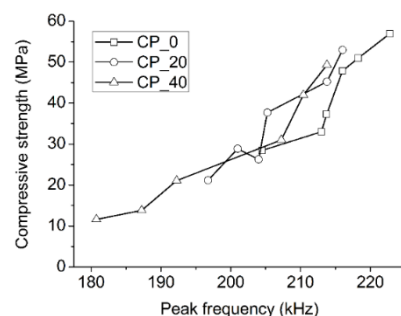


Fig. 12 Peak frequency vs compressive strength

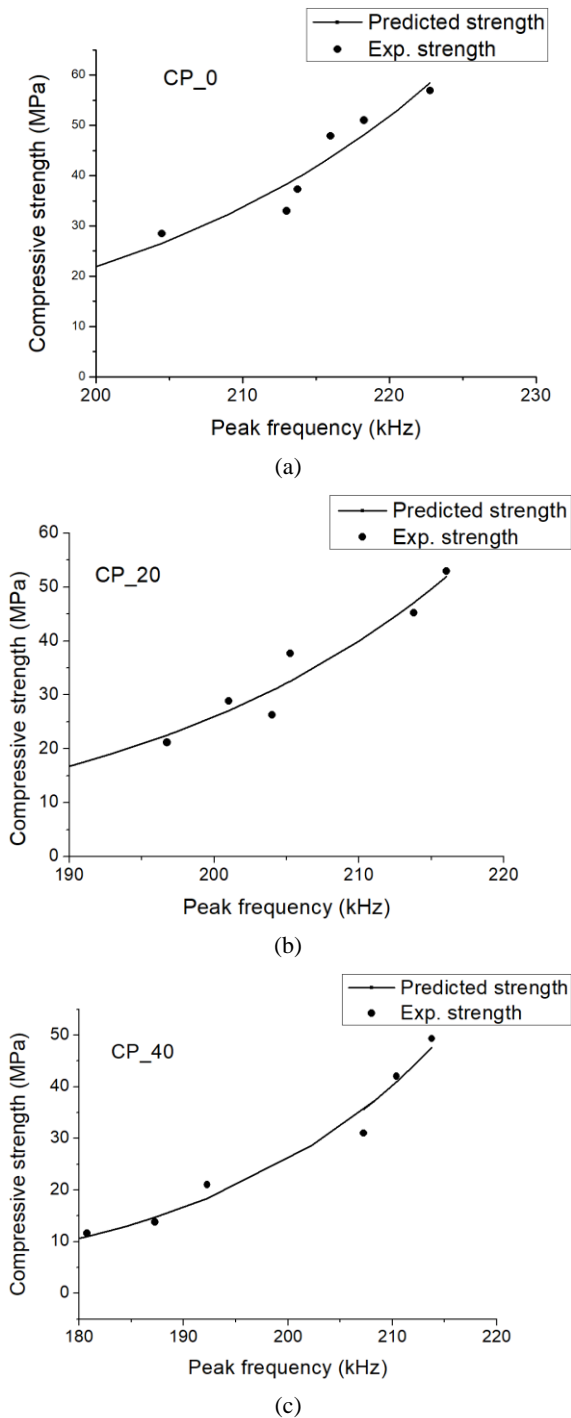


Fig. 13 Correlation between compressive strength and peak frequency (a) CP_0; (b) CP_20; (c) CP_40

the transducers to the specimen surface. Direct transmission method i.e., transducers placed on opposite faces in the cement composite specimens was used for travel time measurement.

After 5 hours of casting, sides of the steel moulds were removed leaving the bottom portion undisturbed. Waveform generator (Keysight 33500B) was used to generate 3-cycle sinusoidal burst signal of 10 V (peak to peak, denoted as pp) amplitude. Then, it was amplified to 50 V pp using two channel isolated amplifier (Keysight 33502A) and fed into

the specimen through transmitting transducer. The ultrasonic signal received at the receiving end was captured by the digital oscilloscope (Keysight InfiniiVision DSOX4024A). The input signals before and after amplification were also visualized through oscilloscope. Finally, oscilloscope was connected to a computer from where waveform generator was controlled and digitized signals were captured and stored. Experimental setup is represented in Fig. 14. A consistent input frequency of 75 kHz is used in the present study.

Fig. 15 shows the calculated ultrasonic wave velocity values in cement composites during hardening. From the wave velocity evolution curves, three typical stages can be categorised: (1) fast-varying, (2) slow-varying and (3) invariable. Separation of three stages can be provided by two critical points, A and B. Points A and B for different composite mixes are provided in Table 3. Compared to mixes CP_0 and CP_20, CP_40 has early appeared point A and lowest velocity value. Point B occurs very soon in CP_0 and beyond that curve remains almost stable. Whereas in CP_20, point B occurs late compared to that in CP_0. This phenomenon is attributed to the nature of hydration reaction in cement blended fly ash system, i.e., inactive pozzolanic reactions which retards the early

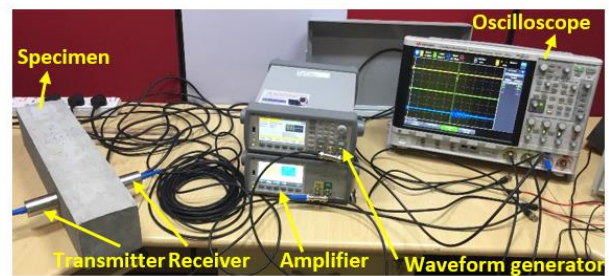


Fig. 14 Ultrasonic wave velocity test setup

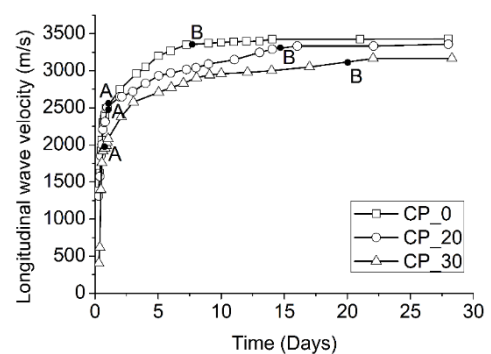


Fig. 15 Ultrasonic wave velocity measured in different composites

Table 3 Critical points for different mixes

Mix	A (days)	B (days)
CP_0	1	7.5
CP_20	1	14.5
CP_40	0.7	20

hydration (Marsh and Day 1988, Mohanraj *et al.* 2010, Kondraivendhan and Bhattacharjee 2015, Hemalatha and Sasmal 2018). In blended system, hydration rate is very low compared to pure cement paste (CP_0) due to slowly reacting fly ash particles and thus, make the slow increase in velocity for prolonged period; hence point B occurs later. In addition, higher replacement of fly ash (CP_40) further decelerates the hydration reaction leading to late occurrence of plateau as compared with CP_20. This implies that slower pozzolanic reaction continues for longer duration, and hence, the microstructure development prolongs (Lu *et al.* 2015).

With the velocity values obtained at different time intervals, dynamic modulus of elasticity is calculated using expression (Qin and Li 2008)

$$E_d = \rho v^2 \tag{7}$$

where v is the longitudinal wave velocity and ρ is the density of the cement composite.

The measured density values of blended cement composites are tabulated in Table 4. The calculated dynamic modulus values are shown in Fig. 16. Experimentally obtained static modulus (E) values at different ages are also presented in the same figure. From this, it is observed that dynamic modulus is higher than the static modulus in most of the cases. Similar observation is made in the earlier works (Popovics *et al.* 2008, Diógenes *et al.* 2011, Salman and Al-Amawee 2018).

Dynamic modulus of elasticity of concrete, E_d is related to the strength using the following relation as proposed by ACI-318 (1995)

$$E_d = K \sqrt{f_{cu}} \tag{8}$$

where f_{cu} is the compressive strength and K is the proportionality constant.

Table 4 Density values of the composite mixes

Mix	Density (kg/m ³)
CP_0	2145
CP_20	2000
CP_40	1850

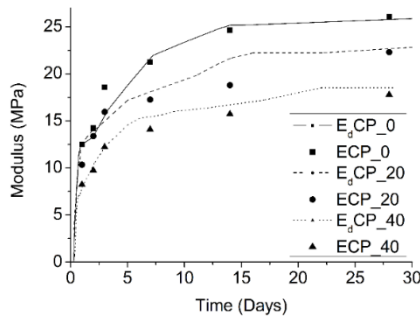


Fig. 16 Dynamic modulus values (E_d) calculated from ultrasonic wave propagation method and static modulus (E) measured from experiments (compression test)

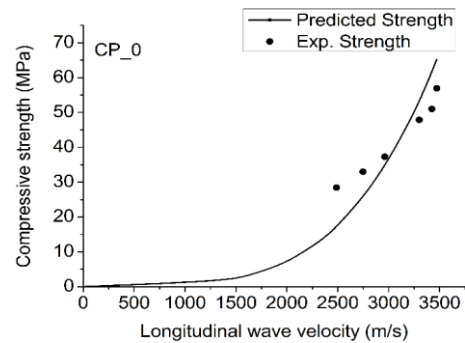
From Eqs. (7) and (8), compressive strength can be correlated to longitudinal wave velocity as follows

$$f_{cu} = \left(\frac{\rho v^2}{K} \right)^2 \tag{9}$$

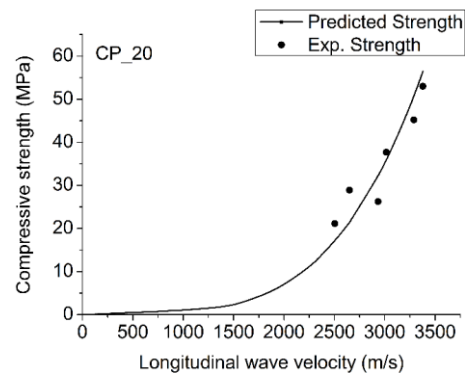
For determining the strength of blended cement composite system i.e., cement paste system with different levels of replacement, a correction factor, p is introduced so

Table 5 ‘p’ value of different mixes

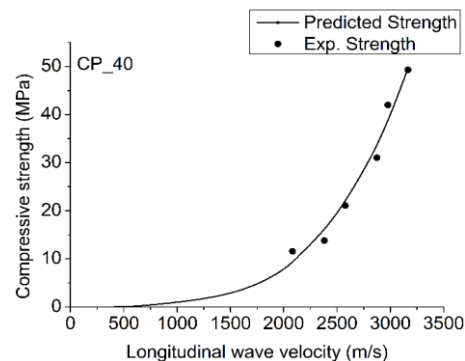
Mix	‘p’ value
CP_0	1
CP_20	0.95
CP_40	0.82



(a)



(b)



(c)

Fig. 17 Strength prediction based on ultrasonic wave propagation (a) CP_0; (b) CP_20; (c) CP_40

that term ‘K’ can be replaced by ‘pK’. From the experimentally obtained longitudinal velocity values at different ages of curing, constant ‘K’ is determined to be 3.201 by curve fitting. Value ‘p’ depends on the percent of fly ash replacement as given in Table 5. Fig. 17 compares the strength predicted using the above expression with the experimental strength values. Comparison shows that for all the mixes, predicted strength using the above expression does show a difference with the experimentally derived data, especially in CP_0 and CP_20 mixes. Predicted strength is seen to be lesser than the actual experiments in the early age, beyond which it reverses.

4.3 Comparison of predicted strength from EMI with UPV

To examine the efficacy of the EMI technique for indirect evaluation of strength in fly ash incorporated cement system, destructive compression test results as well as the evaluated values from ultrasonic wave velocity are

used. Fig. 18 presents the comparison between the strength predicted using EMI technique, with the ultrasonic technique and with those of actual compressive strength obtained from experiments. Comparing EMI and UPV based technique, the analytical model based on UPV underestimates the early age strength i.e., till day 3 and also beyond that it actually overestimates the strength especially in CP_0 and CP_20 specimens.

Further, to quantify the performance of different methods for strength monitoring, most widely used statistical metrics are considered. The error indices used to quantify and summarize the performance of methods are (i) root mean square of percentage error (RMSE) and (ii) mean absolute percentage error (MAPE).

Error indices are defined as follows (Verma *et al.* 2017)

$$RMSE = \sqrt{\frac{1}{n} \sum_{i=1}^n (y_i - x_i)^2} \tag{10}$$

$$MAPE = \frac{1}{n} \sum_{i=1}^n \left| \frac{x_i - y_i}{y_i} \right| \tag{11}$$

where y, x are the experimental and predicted strength values.

The RMSE and MAPE evaluated are shown in Fig. 19. Here the experimental strength was directly evaluated through compression tests and the predicted strength was derived from closed form relations reported for UPV and proposed relations for EMI. Error indices obtained from

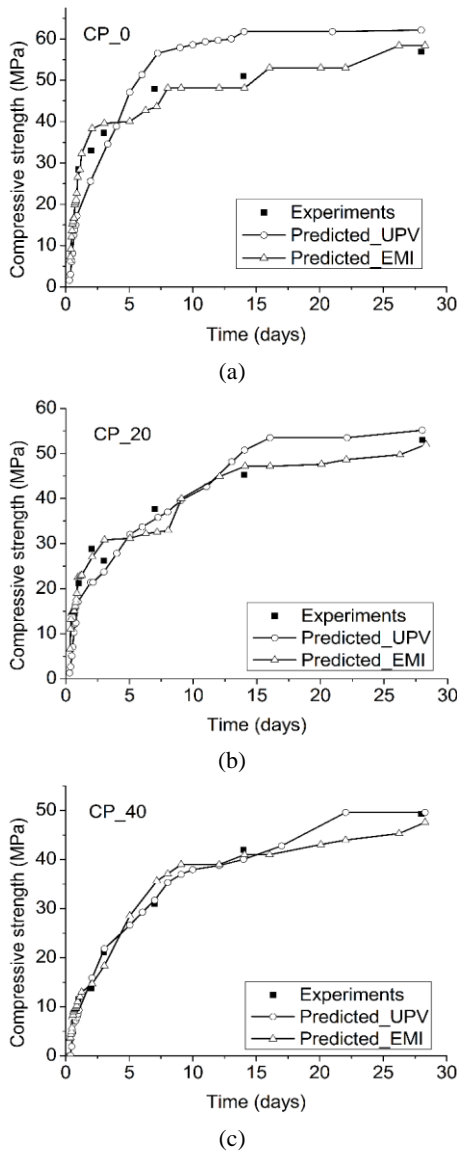


Fig. 18 Strength prediction results from different methods (a) CP_0; (b) CP_20; (c) CP_40

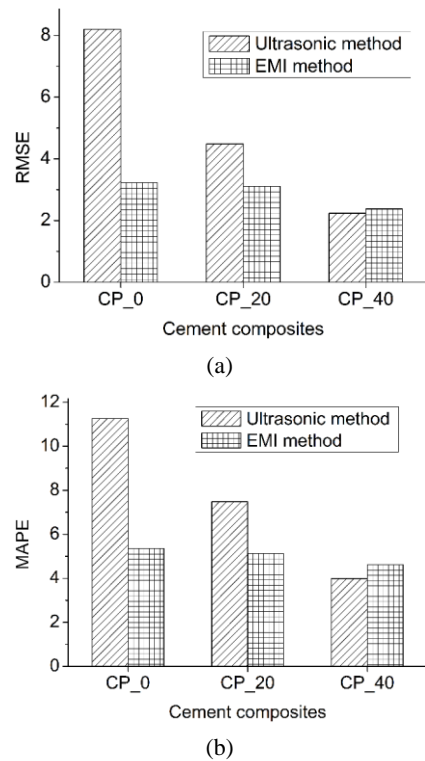


Fig. 19 Comparison of error indices calculated between predicted strength values from UPV and EMI with the destructive compression test

both the methods (RMSE and MAPE) for consistently emphasize that the proposed EMI technique is superior to predict the strength in comparison with the ultrasonic technique.

5. Relationship between stiffness and strength gain (using EMI technique) in hydrating cement system

Predicting the strength gain helps to get first information on the quality of the concrete during construction and service life. Working in that direction, investigations are carried out to correlate the strength from the obtained admittance signature with the observed peak frequency at different ages of curing. To explore the relationship between the strength gain with the stiffness obtained from EMI based impedance measurement, the same is calculated and shown in Fig. 20. Stiffness variation in the hydrating cement composite medium is also explored in section 4.1. Strength gain index is computed by normalizing the compressive strength at different ages of curing with the 28-day compressive strength and stiffness gain index is computed by normalizing the stiffness value at each curing age with the stiffness obtained at 28-day.

It is interesting to note that strength gain and stiffness gain are simultaneous till 3rd day after which strength gain significantly reduces for CP_0 and CP_20. On the other hand, after 3rd day, strength gain in CP_40 is much faster than stiffness gain. Development of rate of stiffness gain is found to be faster than that of strength gain and it is found to have a rapid increase in the first day and a reduction in the following days. For example, in CP_40, strength gain is observed to be 0.25 and corresponding stiffness gain is found to be 0.75 on day 1. Similarly, the same specimen exhibited the strength gain of 0.35 against the stiffness gain of 0.85 on 3rd day. It is also seen that for both stiffness and strength gain, greater amount of shift occurs from day 3 to day 14, whereas the shift from day 14 to day 28 is not significant. This is consistently observed in all specimens, irrespective of the mix type, that EMI technique is a potential tool to monitor the strength gain in any kind of cement system. Correlation between strength and stiffness gain indices recommends that stiffness gain provides a trustworthy sign to better monitor the strength gain especially in case of quality assessment during construction and service too.

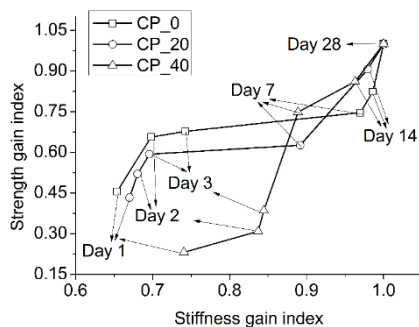


Fig. 20 Stiffness gain index versus strength gain index

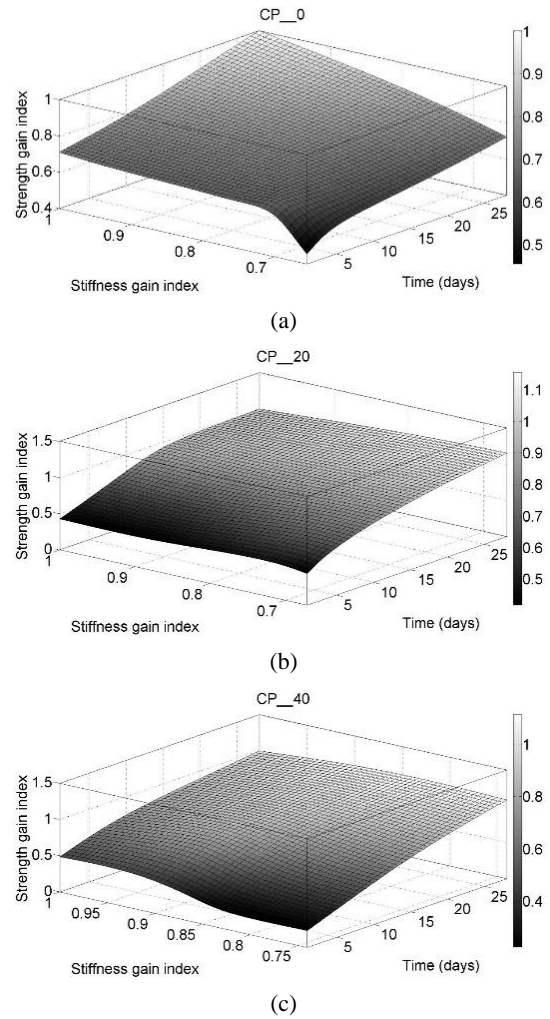


Fig. 21 Thin plate spline surfaces for cement composite systems. (a) CP_0; (b) CP_20; (c) CP_40

Further, most widely used thin plate splines are used for the development of smooth surface from the known stiffness gain at different curing ages to predict the strength gain (see Fig. 21). Knowing the stiffness gain which is obtained from measured admittance signatures, strength gain can be obtained, from which the strength achieved at different curing age can be evaluated.

6. Conclusions

This paper demonstrate the application of EMI technique for deriving strength and stiffness properties of blended (fly ash blended) cement composite systems during hardening. It is also attempted to indirectly evaluate the strength gain in cement system using EMI technique. The same is validated with strength directly evaluated from destructive compression experiments and also compared with the commonly used ultrasonic wave velocity based technique. From the present study, the following key observations are made:

- (i) In low frequency range of 50-100 kHz, cement system behaves similar to Kelvin-Voigt system

- (parallel combination of spring and damper).
- (ii) Computed local stiffness of equivalent system is found to increase consistently with hydration. The same is identified as a suitable indicator to predict the stiffness gain when the cement system gets hardened.
 - (iii) From the shift of peak frequency that is noticed in admittance measurement during hardening, an empirical relation is proposed to estimate the strength at different ages of curing of fly ash blended cement system.
 - (iv) The proposed EMI based strength estimation models could effectively be used in monitoring the strength development at different ages of curing of fly ash blended cement system.
 - (v) Error indices obtained from RMSE and MAPE revealed that the strength prediction based on EMI based wave propagation technique is better than commonly used UPV technique.
 - (vi) An attempt is made, for the first time, to relate the strength and stiffness gain index with the age of curing of blended cement system which helps enormously in identifying the strength gained at different ages; and a very good and consistent correlation is observed between the strength and stiffness gain indices.

The present study provides a smart technique to monitor the strength (and stiffness) gain in materials using the EMI signatures from distributed sensing approach. The proposed technique is easy to implement using the inexpensive sensors and can be monitored in real time.

Acknowledgments

The authors would like to acknowledge the members of Special and Multifunctional Structures Laboratory, CSIR-SERC for their help during experiments. Special and sincere thanks to Mr. Rajinikant Rao and Mr. Gautham, PhD scholars, AcSIR, CSIR-SERC for their immense help rendered during continuous impedance measurements.

References

- ACI 318 (1995), Building code requirements for structural concrete and commentary, American Concrete Institute; Farmington Hills, MI, USA.
- ASTM C-09 on Concrete and Concrete Aggregates (2013), Standard specification for coal fly ash and raw or calcined natural pozzolan for use in concrete, ASTM International; PA, USA.
- Bhalla, S. (2004), "A mechanical impedance approach for structural identification, health monitoring and non-destructive evaluation using piezo-impedance transducers", Doctoral Dissertation; Nanyang Technological University, School of Civil & Environmental Engineering, Singapore.
- Bhalla, S., Vittal, P.A. and Veljkovic, M. (2012), "Piezo-impedance transducers for residual fatigue life assessment of bolted steel joints", *Struct. Health Monitor.*, **11**(6), 733-750. <https://doi.org/10.1177%2F1475921712458708>
- Bhalla, N., Sharma, S., Sharma, S. and Siddique, R. (2018), "Monitoring early-age setting of silica fume concrete using wave propagation techniques", *Constr. Build. Mater.*, **162**, 802-815. <https://doi.org/10.1016/j.conbuildmat.2017.12.032>
- Demirboğa, R., Türkmen, İ. and Karakoc, M.B. (2004), "Relationship between ultrasonic velocity and compressive strength for high-volume mineral-admixed concrete", *Cement Concrete Res.*, **34**(12), 2329-2336. <https://doi.org/10.1016/j.cemconres.2004.04.017>
- Diógenes, H.J.F., Cossolino, L.C., Pereira, A.H.A., El Debs, M.K. and El Debs, A.L.H.C. (2011), "Determination of modulus of elasticity of concrete from the acoustic response", *Revista IBRACON de Estruturas e Materiais*, **4**(5), 803-813. <http://dx.doi.org/10.1590/S1983-41952011000500007>
- Galan, A. (1967), "Estimate of concrete strength by ultrasonic pulse velocity and damping constant", *J. Proceedings*, **64**(10), 678-684. <https://doi.org/10.14359/7596>
- Ghafari, E., Yuan, Y., Wu, C., Nantung, T. and Lu, N. (2018), "Evaluation the compressive strength of the cement paste blended with supplementary cementitious materials using a piezoelectric-based sensor", *Constr. Build. Mater.*, **171**, 504-510. <https://doi.org/10.1016/j.conbuildmat.2018.03.165>
- Gül, R., Demirboğa, R. and Güvercin, T. (2006), "Compressive strength and ultrasound pulse velocity of mineral admixed mortars", *Ind. J. Eng. Mater. Sci.*, **13**, 18-24. <http://nopr.niscair.res.in/handle/123456789/7210>
- Hassett, D.J. and Eylands, K.E. (1997), "Heat of hydration of fly ash as a predictive tool", *Fuel*, **76**(8), 807-809. [https://doi.org/10.1016/S0016-2361\(97\)00058-6](https://doi.org/10.1016/S0016-2361(97)00058-6)
- Hemalatha, T. and Sasmal, S. (2018), "Early-age strength development in fly ash blended cement composites: investigation through chemical activation", *Magaz. Concrete Res.*, **71**(5), 260-270. <https://doi.org/10.1680/jmacr.17.00336>
- Huynh, T.C. and Kim, J.T. (2017), "Quantitative damage identification in tendon anchorage via PZT interface-based impedance monitoring technique", *Smart Struct. Syst., Int. J.*, **20**(2), 181-195. <https://doi.org/10.12989/sss.2017.20.2.181>
- Huynh, T.C., Dang, N.L. and Kim, J.T. (2018), "PCA-based filtering of temperature effect on impedance monitoring in prestressed tendon anchorage", *Smart Struct. Syst., Int. J.*, **22**, 57-70. <https://doi.org/10.12989/sss.2018.22.1.057>
- IS 4031 (1968), Methods of Physical Tests for Hydraulic Cement, Part I, Bureau of Indian Standards, New Delhi, India.
- Ji, Q., Ho, M., Zheng, R., Ding, Z. and Song, G. (2015), "An exploratory study of stress wave communication in concrete structures", *Smart Struct. Syst., Int. J.*, **15**(1), 135-150. <https://doi.org/10.12989/sss.2015.15.1.135>
- Kang, M.S., An, Y.K. and Kim, D.J. (2018), "Electrical impedance-based crack detection of SFRC under varying environmental conditions", *Smart Struct. Syst., Int. J.*, **22**(1), 1-11. <https://doi.org/10.12989/sss.2018.22.1.001>
- Kim, J., Kim, J.W. and Park, S. (2014), "Early-Age Concrete Strength Estimation Technique using Embedded Piezoelectric self-sensing impedance", *Proceedings of EWSHM-7th European Workshop on Structural Health Monitoring*, Inria, July.
- Kondraivendhan, B. and Bhattacharjee, B. (2015), "Flow behavior and strength for fly ash blended cement paste and mortar", *Int. J. Sustain. Built Environ.*, **4**(2), 270-277. <https://doi.org/10.1016/j.ijsbe.2015.09.001>
- Lam, L., Wong, Y.L. and Poon, C.S. (2000), "Degree of hydration and gel/space ratio of high-volume fly ash/cement systems", *Cement Concrete Res.*, **30**(5), 747-756. [https://doi.org/10.1016/S0008-8846\(00\)00213-1](https://doi.org/10.1016/S0008-8846(00)00213-1)
- Lee, H.K., Lee, K.M., Kim, Y.H., Yim, H. and Bae, D.B. (2004), "Ultrasonic in-situ monitoring of setting process of high-performance concrete", *Cement Concrete Res.*, **34**(4), 631-640. <https://doi.org/10.1016/j.cemconres.2003.10.012>
- Liang, C., Sun, F.P. and Rogers, C.A. (1997), "Coupled electro-

- mechanical analysis of adaptive material systems-determination of the actuator power consumption and system energy transfer”, *J. Intel. Mater. Syst. Struct.*, **8**(4), 335-343.
<https://doi.org/10.1177/1045389X9400500102>
- Lim, Y.Y., Kwong, K.Z., Liew, W.Y.H. and Soh, C.K. (2016), “Non-destructive concrete strength evaluation using smart piezoelectric transducer—A comparative study”, *Smart Mater. Struct.*, **25**(8), 085021.
<https://doi.org/10.1088/0964-1726/25/8/085021>
- Lin, Y., Lai, C.P. and Yen, T. (2003), “Prediction of ultrasonic pulse velocity (UPV) in concrete”, *Mater. J.*, **100**(1), 21-28.
<https://doi.org/10.14359/12459>
- Lu, Y., Ma, H. and Li, Z. (2015), “Ultrasonic monitoring of the early-age hydration of mineral admixtures incorporated concrete using cement-based piezoelectric composite sensors”, *J. Intel. Mater. Syst. Struct.*, **26**(3), 280-291.
<https://doi.org/10.1177/1045389X14525488>
- Marsh, B.K. and Day, R.L. (1988), “Pozzolanic and cementitious reactions of fly ash in blended cement pastes”, *Cement Concrete Res.*, **18**(2), 301-310.
[https://doi.org/10.1016/0008-8846\(88\)90014-2](https://doi.org/10.1016/0008-8846(88)90014-2)
- Mohammed, B.S. and Adamu, M. (2018), “Non-destructive evaluation of nano silica-modified roller-compacted rubbercrete using combined SonReb and response surface methodology”, *Road Mater. Pavement Des.*, 1-21.
<https://doi.org/10.1080/14680629.2017.1417891>
- Mohanraj, K., Sivakumar, G. and Barathan, S. (2010), “Hydration process of fly ash blended cement composite”, *Int. J. Chem. Sci.*, **8**(1), 589-601.
- Namagga, C. and Atadero, R.A. (2009), “Optimization of fly ash in concrete: High lime fly ash as a replacement for cement and filler material”, *Proceedings of World of Coal Ash Conference (WCCA)*, Lexington, KY, USA, May.
- Neville, A.M. (1995), *Properties of Concrete*, Longman, London, UK.
- Popovics, J.S., Zemajtis, J. and Shkolnik, I. (2008), “A study of static and dynamic modulus of elasticity of concrete”, ACI-CRC Final Report, American Concrete Institute; Farmington Hills, MI, USA.
- Prem, P.R., Thirumalaiselvi, A. and Verma, M. (2019), “Applied linear and nonlinear statistical models for evaluating strength of Geopolymer concrete”, *Comput. Concrete, Int. J.*, **24**(1), 7-17.
<https://doi.org/10.12989/cac.2019.24.1.007>
- Qin, L. and Li, Z. (2008), “Monitoring of cement hydration using embedded piezoelectric transducers”, *Smart Mater. Struct.*, **17**(5), 055005. <https://doi.org/10.1088/0964-1726/17/5/055005>
- Qixian, L. and Bungey, J.H. (1996), “Using compression wave ultrasonic transducers to measure the velocity of surface waves and hence determine dynamic modulus of elasticity for concrete”, *Constr. Build. Mater.*, **10**(4), 237-242.
[https://doi.org/10.1016/0950-0618\(96\)00003-7](https://doi.org/10.1016/0950-0618(96)00003-7)
- Quinn, W., Kelly, G. and Barrett, J. (2012), “Development of an embedded wireless sensing system for the monitoring of concrete”, *Struct. Health Monitor.*, **11**(4), 381-392.
<https://doi.org/10.1177%2F1475921711430438>
- Rajabi, M., Shamshirsaz, M. and Naraghi, M. (2017), “Crack detection in rectangular plate by electromechanical impedance method: modeling and experiment”, *Smart Struct. Syst., Int. J.*, **19**(4), 361-369. <https://doi.org/10.12989/sss.2017.19.4.361>
- Şahmaran, M., Yaman, Ö. and Tokyay, M. (2007), “Development of high-volume low-lime and high-lime fly-ash-incorporated self-consolidating concrete”, *Magaz. Concrete Res.*, **59**(2), 97-106. <https://doi.org/10.1680/mac.2007.59.2.97>
- Sakai, E., Miyahara, S., Ohsawa, S., Lee, S.H. and Daimon, M. (2005), “Hydration of fly ash cement”, *Cement Concrete Res.*, **35**(6), 1135-1140.
<https://doi.org/10.1016/j.cemconres.2004.09.008>
- Salman, A.P.D.M.M. and Al-Amawee, E.A.H. (2018), “The ratio between static and dynamic modulus of elasticity in normal and high strength concrete”, *J. Eng. Sustain. Develop.*, **10**(2), 163-174.
- Saravanan, T.J., Balamonica, K., Priya, C.B., Reddy, A.L. and Gopalakrishnan, N. (2015), “Comparative performance of various smart aggregates during strength gain and damage states of concrete”, *Smart Mater. Struct.*, **24**(8), 085016.
<https://doi.org/10.1088/0964-1726/24/8/085016>
- Saravanan, T.J., Balamonica, K., Bharathi Priya, C., Gopalakrishnan, N. and Murthy, S.G.N. (2017), “Piezoelectric EMI-based monitoring of early strength gain in concrete and damage detection in structural components”, *J. Infrastruct. Syst.*, **23**(4), 04017029.
[https://doi.org/10.1061/\(ASCE\)IS.1943-555X.0000386](https://doi.org/10.1061/(ASCE)IS.1943-555X.0000386)
- Sata, V., Jaturapitakkul, C. and Kiattikomol, K. (2007), “Influence of pozzolan from various by-product materials on mechanical properties of high-strength concrete”, *Constr. Build. Mater.*, **21**(7), 1589-1598.
<https://doi.org/10.1016/j.conbuildmat.2005.09.011>
- Shafiq, N. (2011), “Degree of hydration and compressive strength of conditioned samples made of normal and blended cement system”, *KSCE J. Civil Eng.*, **15**(7), 1253.
<https://doi.org/10.1007/s12205-011-1193-x>
- Shin, S.W., Qureshi, A.R., Lee, J.Y. and Yun, C.B. (2008), “Piezoelectric sensor based nondestructive active monitoring of strength gain in concrete”, *Smart Mater. Struct.*, **17**(5), 055002.
<https://doi.org/10.1088/0964-1726/17/5/055002>
- Sofi, M., Lumantarna, E., Zhou, Z., San Nicolas, R. and Mendis, P. (2017), “From Hydration to Strength Properties of Fly Ash Based Mortar”, *J. Mater. Sci. Chem. Eng.*, **5**(12), 63.
<https://doi.org/10.4236/msce.2017.512006>
- Soh, C.K. and Bhalla, S. (2005), “Calibration of piezo-impedance transducers for strength prediction and damage assessment of concrete”, *Smart Mater. Struct.*, **14**(4), 671.
<https://doi.org/10.1088/0964-1726/14/4/026>
- Talakokula, V., Bhalla, S. and Gupta, A. (2018), “Monitoring early hydration of reinforced concrete structures using structural parameters identified by piezo sensors via electromechanical impedance technique”, *Mech. Syst. Signal Process.*, **99**, 129-141.
<https://doi.org/10.1016/j.ymsp.2017.05.042>
- Tanesi, J. and Ardani, A. (2013), “Isothermal Calorimetry as a Tool to Evaluate Early-Age Performance of Fly Ash Mixtures”, *Transportation Research Record*, **2342**(1), 42-53.
<https://doi.org/10.3141/2342-06>
- Tawie, R. and Lee, H.K. (2010), “Monitoring the strength development in concrete by EMI sensing technique”, *Constr. Build. Mater.*, **24**(9), 1746-1753.
<https://doi.org/10.1016/j.conbuildmat.2010.02.014>
- Tharmaratnam, K. and Tan, B.S. (1990), “Attenuation of ultrasonic pulse in cement mortar”, *Cement Concrete Res.*, **20**(3), 335-345.
[https://doi.org/10.1016/0008-8846\(90\)90022-P](https://doi.org/10.1016/0008-8846(90)90022-P)
- Thomas, M.D.A. (2007), “Optimizing the use of fly ash in concrete (Vol. 5420)”, Skokie, IL: Portland Cement Association.
- Trtnik, G., Kavčič, F. and Turk, G. (2009), “Prediction of concrete strength using ultrasonic pulse velocity and artificial neural networks”, *Ultrasonics*, **49**(1), 53-60.
<https://doi.org/10.1016/j.ultras.2008.05.001>
- Verma, M., Thirumalaiselvi, A. and Rajasankar, J. (2017), “Kernel-based models for prediction of cement compressive strength”, *Neural Comput. Applicat.*, **28**(1), 1083-1100.
<https://doi.org/10.1007/s00521-016-2419-0>
- Wang, D. and Zhu, H. (2011), “Monitoring of the strength gain of concrete using embedded PZT impedance transducer”, *Constr. Build. Mater.*, **25**(9), 3703-3708.
<https://doi.org/10.1016/j.conbuildmat.2011.04.020>
- Wang, D., Song, H. and Zhu, H. (2014), “Embedded 3D

- electromechanical impedance model for strength monitoring of concrete using a PZT transducer”, *Smart Mater. Struct.*, **23**(11), 115019. <https://doi.org/10.1088/0964-1726/23/11/115019>
- Wolfs, R.J.M., Bos, F.P. and Salet, T.A.M. (2018), “Correlation between destructive compression tests and non-destructive ultrasonic measurements on early age 3D printed concrete”, *Constr. Build. Mater.*, **181**, 447-454. <https://doi.org/10.1016/j.conbuildmat.2018.06.060>
- Yoon, H., Kim, Y., Kim, H., Kang, J. and Koh, H.M. (2017), “Evaluation of early-age concrete compressive strength with ultrasonic sensors”, *Sensors*, **17**(8), 1817. <https://doi.org/10.3390/s17081817>
- Zhang, S., Zhang, Y. and Li, Z. (2018), “Ultrasonic monitoring of setting and hardening of slag blended cement under different curing temperatures by using embedded piezoelectric transducers”, *Constr. Build. Mater.*, **159**, 553-560. <https://doi.org/10.1016/j.conbuildmat.2017.10.124>
- Zheng, Y., Chen, D., Zhou, L., Huo, L., Ma, H. and Song, G. (2018), “Evaluation of the effect of fly ash on hydration characterization in self-compacting concrete (SCC) at very early ages using piezoceramic transducers”, *Sensors*, **18**(8), 2489. <https://doi.org/10.3390/s18082489>